Title

Stragegies to Detect Hidden Geothermal Systems Based on Monitoring and Analysis of CO2 in
the Near-Surface Environment

Permalink
https://escholarship.org/uc/item/88m1f9h4

Authors

Lewicki, Jennifer L.
Oldenburg, Curtis M.

Publication Date
2008-06-16

Peer reviewed

Strategies to Detect Hidden Geothermal Systems Based on Monitoring and Analysis of CO_2 in the Near-Surface Environment

Jennifer L. Lewicki[a,*] and Curtis M. Oldenburg[a]

[a] Earth Sciences Division, Lawrence Berkeley National Laboratory, 1 Cyclotron Road,

Berkeley, CA 94720, USA

* Corresponding author. Fax: 510-486-5686; E-mail address: jllewicki@lbl.gov

Abstract

We investigate the potential for CO_2 monitoring in the near-surface environment as an approach to exploration for hidden geothermal systems. Numerical simulations of CO_2 migration from a model hidden geothermal system show that CO_2 concentrations can reach high levels in the shallow subsurface even for relatively low CO_2 fluxes. Therefore, subsurface measurements offer an advantage over above-ground measurements which are affected by winds that rapidly disperse CO_2. To meet the challenge of detecting geothermal CO_2 emissions within the natural background variability of CO_2, we propose an approach that integrates available detection and monitoring techniques with statistical analysis and modeling.

Keywords: Hidden geothermal system; Exploration; carbon dioxide; flux; concentration; Numerical simulation; Statistics; Basin and Range

1. Introduction

Worldwide, most commercial geothermal projects have been developed in or near areas of surface manifestations (e.g., hot springs, geysers, fumaroles). Also, the majority of hydrothermal systems with obvious surface expressions in the U.S. have been explored to determine their development potential. Discovery of new geothermal systems will therefore require exploration of areas where the resources are either hidden or lie at greater depths than presently known reservoirs. As a result, research must be geared toward the development of novel exploration techniques to locate these less-obvious geothermal systems.

We define "hidden" geothermal systems as those with no apparent surface features. Emissions of moderate-to-low solubility gases (e.g., CO_2, He, CH_4) may be one of the primary near-surface signals from these systems. Therefore, the detection of anomalous gas emissions related to hidden geothermal systems may be an important tool to discover new resources (Klusman et al., 2000). We focus our study on the detection and monitoring of CO_2 in the near-surface environment as an approach to discover hidden geothermal systems because (1) CO_2 is the major non-condensible gas present in geothermal systems (e.g., Ellis and Mahon, 1977), (2) due to its moderate solubility in water, CO_2 from volcanic-hydrothermal sources tends to migrate to the near-surface in the gaseous phase in equal or greater proportion than dissolved in groundwater (e.g., Cruz et al., 1999; Favara et al., 2001; Evans et al., 2002), and (3) a broad range of technologies is available to monitor CO_2 in the near-surface environment. Importantly, however, CO_2 is produced in the near surface by a variety of biologic and hydrologic processes, and identifying CO_2 from hidden geothermal resources will involve monitoring a system with large variation in fluxes and concentrations arising from these processes. The detection of anomalous CO_2 will therefore require searching for potential geothermal anomalies, likely of small magnitude, over areas of tens of km^2 or more within the varying background CO_2 fluxes and concentrations. Here, we present integrated measurement, modeling, and analysis strategies designed to meet this challenge.

2. CO_2 in known volcanic and hydrothermal systems

Numerous diffuse CO_2 degassing studies have been conducted in known (i.e., "visible") volcanic and hydrothermal environments, many of which focused on characterizing the magnitude and spatial distribution of CO_2 emissions. Table 1 summarizes the maximum (and average, if applicable) surface CO_2 fluxes and soil CO_2 concentrations measured in selected known systems. As shown, the maximum CO_2 fluxes and concentrations measured varied widely, but could reach up to ~75,000 g $m^{-2}d^{-1}$ and 90 vol.%, respectively. Both elevated CO_2 fluxes and concentrations were commonly associated with faults, fractures, and eruptive fissures within the study areas. While surface CO_2 emission rates from hidden geothermal systems will likely be lower than those measured in known volcanic and hydrothermal systems, the preferential pathways for CO_2 flow from depth to the near surface should be similar.

3. Simulations of geothermal CO_2 migration

We conducted numerical simulations to evaluate the magnitudes and spatial distribution of anomalous near-surface CO_2 concentrations and fluxes that might result when CO_2 leaks from a hidden geothermal system at depth. These simulations were carried out to provide information we can then use to design and evaluate potential detection and monitoring methods.

We use the numerical code T2CA (Oldenburg and Unger, 2004), a research module of TOUGH2 (Pruess et al., 1999). T2CA retains the fundamental porous media flow and transport capabilities of TOUGH2, and models five components (water, brine, CO_2, a gas tracer, and air) under isothermal or non-isothermal conditions. The main advance in T2CA is the implementation of a simple atmospheric transport and dispersion capability for dilute gases based on the variable-K theory (Arya, 1999). That is, a constant time-averaged logarithmic wind velocity profile is specified for advection above the ground surface, and atmospheric dispersion is modeled as a diffusion process with variable diffusivity as a function of height. In this way, T2CA models coupled subsurface and atmospheric surface layer gas flow and transport.

The geologic framework of the modeled hidden geothermal system is based loosely on an arid Basin and Range Province system like the Dixie Valley (Nevada) geothermal system, only without any surface manifestations. In particular, we consider a two-dimensional system in which an alluvial fan covers a geothermal anomaly associated with deep range-bounding faults so that it is essentially invisible at the surface (Fig. 1). Within this system, we model the upward migration of CO_2 from a small (15 m^2) region that represents the top of a conductive fault, located near the water table. The CO_2 spreads in the heterogeneous system (i.e., the alluvial fan) as it migrates upward until it seeps out at the ground surface. The grid consists of 67 15-m gridblocks in the *x*-direction, and 31 4-m gridblocks in the *z*-direction. We do not consider the effects of infiltration of meteoric water to simplify models and focus attention on arid Basin and Range-type environments. Additional properties of the system are presented in Table 2.

We consider both a homogeneous permeability case, along with five realizations of heterogeneous permeability generated using simulated annealing. The heterogeneous permeability cases are significant because gas migration will tend to follow high-permeability pathways. Here, permeability is characterized by a mean value of 10^{-12} m^2, and varies by four orders of magnitude. There is a 45-m correlation length in the *x*-direction, and no correlation in the z-direction, thereby creating a layered structure intended to represent an alluvial fan. We simulated source strength CO_2 fluxes of 5.76, 57.6 and 576 g m^{-2} d^{-1} which will produce much smaller surface fluxes as the CO_2 spreads during migration from the source region to the ground surface. For reference, the largest source CO_2 flux we consider is similar to the highest surface CO_2 fluxes measured at Dixie Valley (Table 1). The source fluxes were arbitrarily chosen to produce small CO_2 seepage fluxes, and are significantly lower than those measured in known/visible volcanic and hydrothermal systems (e.g., Table 1). We chose to model this low range of values to test the limits of available technologies for near-surface CO_2 detection. We present results for 200 years of simulation, at which point the gas seepage flux and concentrations are nearly steady.

To emphasize the key simulation results relevant to design of a near-surface CO_2 monitoring program, we present coupled CO_2 subsurface migration and surface-layer mixing for one of our five heterogeneous permeability realizations, high source CO_2 flux, and constant wind speeds of 1 and 3 m s^{-1} (Fig. 2). Figure 2 shows that the gas in the plume is essentially pure CO_2 in the subsurface, even though the source CO_2 flux is quite small. Conversely, surface-layer CO_2 concentrations only reach maximum values of ~10^{-6} mole fraction (1 ppmv) for both wind speeds considered, indicating that surface-layer winds are capable of diluting CO_2 concentrations to very small values above the ground surface. For reference, natural ambient CO_2 concentration is approximately 360 ppmv. We note that stagnant conditions and topographic depressions are moderating effects that could allow higher CO_2 concentrations to develop, although these effects are not modeled here. In general, under low to moderate wind speed conditions, the relatively high simulated CO_2 concentrations observed at the ground surface and in the subsurface suggest that monitoring of CO_2 in these regions may have greater potential to detect anomalous CO_2 of geothermal origin than above-ground techniques.

Figure 3 shows horizontal profiles of CO_2 concentration at 3 m depth and surface CO_2 flux for the low, medium, and high source CO_2 fluxes and one heterogeneous permeability realization. These profiles all show a similar increase and then decrease in concentration and flux crossing the CO_2 plume. Maximum CO_2 concentrations for the low, medium, and high source strengths are about 2 x 10^4, 2 x 10^5 and 7 x 10^5 ppmv, respectively, whereas maximum surface CO_2 fluxes are about 4 x 10^{-4}, 0.52, and 100 g m^{-2} d^{-1}, respectively. These profiles also show that the width of the CO_2 plume increases with increasing source strength. If the source area of CO_2 emission were increased (i.e., to simulate more diffuse, rather than focused CO_2 flow), the magnitude of the near-surface CO_2 concentration and flux signals would decrease, while the width of the anomaly would increase. Relative to the homogeneous permeability cases (not shown here), fluxes along the heterogeneous profiles are more spatially variable and maximum observed fluxes may be greater or lower, depending on whether high or low permeability was assumed, respectively. Complete results for the five heterogeneous permeability realizations, homogeneous permeability, and three source CO_2 flux values can be found in Lewicki and Oldenburg (2004).

4. Background CO_2

We define "background" CO_2 as CO_2 derived mainly from the atmosphere and biologically mediated oxidation of organic carbon. Background soil CO_2 fluxes and concentrations are primarily dependent on CO_2 production in the soil by biological processes, flow of CO_2 from biologic/hydrologic sub-soil sources into the soil column, and exchange of CO_2 with the atmosphere by concentration and pressure-driven transport processes (diffusion and advection, respectively).

Biologically produced CO_2 in soils (i.e., soil respiration) is derived from root respiration and oxidative decay of organic matter. While many factors may regulate soil respiration rates, changes in atmospheric and soil temperature and soil moisture have been shown to strongly influence these rates and related CO_2 concentrations and fluxes (e.g., Wiant, 1967a; Wiant 1967b; Kucera and Kirkham, 1971; Alexander, 1977; Amundson and Smith, 1988; Osozawa and Hasegawa, 1995). CO_2 that enters soil from sub-soil sources can be derived from groundwater degassing of CO_2 that in turn was derived from respiration, atmospheric, and carbonate mineral sources. Also, production of CO_2 at sub-soil depths can occur by oxidative decay of relatively young or ancient (peat, lignite, kerogen) organic matter in the vadose zone. Exchange of CO_2 from subsurface sources with the atmosphere can occur by diffusion and/or advection. Diffusive flow depends on the gas production rate and soil temperature, moisture, and properties such as porosity. Advective flow can be driven by changes in atmospheric temperature, pressure, wind, and rainfall (e.g., Schery et al., 1984; Hinkle 1994; Massmann and Farrier, 1992; Lewicki et al., 2003b).

The chemical and isotopic compositions of gases collected at soil and sub-soil depths provides information on CO_2 production and the source of this CO_2 (Table 3). CO_2 concentration profiles measured as a function of depth in the vadose zone can yield information about CO_2 production. For example, an increase in CO_2 concentration with depth below the soil indicates CO_2 production at sub-soil depths. Production of CO_2 by oxidative decay of organic matter tends to consume O_2 at a similar rate. Also, atmospheric O_2 will diffuse down into the soil and sub-soil as subsurface CO_2 diffuses to the atmosphere. A flux of geothermal CO_2 would produce elevated CO_2 concentration at depth, relative to the atmosphere, but would not be accompanied by O_2 consumption, although atmospheric O_2 would diffuse down into the soil. Based on these general processes, the CO_2 and O_2 concentration profiles should be different, depending on whether a geothermal flux is present. One might expect groundwater degassing of respiration and atmospheric-derived CO_2 to show similar chemical trends within the vadose zone to degassing of geothermal CO_2. However, vadose zone CO_2 concentrations produced by groundwater degassing and biological respiration processes have generally been reported to be less than 13 vol.% CO_2 (e.g., Wood and Petraitis, 1984; Amundson and Davidson, 1990; Wood et al., 1993), whereas near-surface CO_2 concentrations associated with geothermal emissions could be much higher. For example, simulated geothermal source CO_2 fluxes of 57.6 to 576 g m^{-2} d^{-1} produce maximum near-surface CO_2 concentrations of ~20–70 vol.% (2 x 10^5 to 7 x 10^5 ppmv, Fig. 3). Importantly, however, the maximum near-surface CO_2 concentration produced by a source CO_2 flux of 5.76 g $m^{-2}d^{-1}$ is only predicted to be ~2 vol.% (2 x 10^4 ppmv, Fig. 3), which could be problematic to distinguish from background CO_2 concentrations. Table 3 also shows that the ranges of typical carbon isotopic compositions of geothermal CO_2 are distinct from those whose dominant sources are background biological CO_2. Here, carbon-13 values are reported as $\delta^{13}C$, the deviation in parts per thousand (‰) of the $^{13}C/^{12}C$ ratio in the sample from that of the Pee Dee Belemnite (PDB) reference standard. Carbon-14 values are reported as $\Delta^{14}C$, the deviation, in parts per thousand of the $^{14}C/^{12}C$ ratio in the sample from that of the reference standard (oxalic acid decay corrected to 1950). Analysis of the $\Delta^{14}C$ and $\delta^{13}C$ compositions of gases collected from the soil and, in particular, from the sub-soil where biologic CO_2 production rates are low can serve as a tool to distinguish between CO_2 of geothermal and background origins.

5. Instrumentation for monitoring CO_2

A broad range of technologies is available to measure near-surface CO_2 concentrations and fluxes to detect anomalous CO_2 of geothermal origin. These technologies include (1) the infrared gas analyzer (IRGA) for measurement of concentrations at point locations, (2) the accumulation chamber (AC) method for measuring soil CO_2 fluxes at point locations, (3) the eddy covariance (EC) method for measuring net CO_2 flux over a given area, (4) hyperspectral imaging of vegetative stress resulting from elevated CO_2 concentrations, and (5) light detection and ranging (LIDAR) that can measure CO_2 concentrations over an integrated path in the air column. These techniques differ from one another in terms of the spatial and temporal scale of the measurement, measurement sensitivity and error, and cost. Here, we focus on the relatively low-cost and reliable IRGA, AC, and EC methods for CO_2 concentration and flux measurements.

5.1. Infrared gas analyzer

The infrared gas analyzer (IRGA) is an instrument commonly used to measure CO_2 concentration in subsurface or atmospheric air. The measurement is based on CO_2 absorption of infrared radiation. Portable IRGAs are available for use in the field and can make single or continuous measurements over time; each measurement is made within about one second to minutes, depending on the instrument. IRGAs are available to measure CO_2 concentration over a low range (e.g., 0-1000 ppmv) or over a high range (e.g., 0-100 vol.%). The precision and accuracy can be as good as ± 0.2 ppmv at 350 ppmv and ± 1%, respectively. The cost of equipment may range from ~\$500 to \$30,000.

Soil or subsoil gas CO_2 concentrations can be rapidly measured at many point locations within a large area using a probe and a portable IRGA. Using this method, a probe is driven down to the depth of interest, gas is pumped from the soil or sub-soil into the IRGA by an internal pump, and CO_2 concentration is measured.

5.2. Accumulation chamber method

IRGAs may be coupled with additional instrumentation to obtain surface CO_2 fluxes. For example, the accumulation chamber (AC) method (e.g., Chiodini et al., 1998) is used to measure soil CO_2 flux using an AC and an IRGA. An AC with an open bottom (cm^2 scale) is placed on the soil surface, the contained air is circulated through the AC and the IRGA, and the rate of change of CO_2 concentration in the AC is measured by the IRGA (Fig. 4). The flux of CO_2 (F) is then calculated according to

$$F = \left(\frac{\rho V}{A}\right)\left(\frac{d[CO_2]}{dt}\right) \tag{1}$$

where ρ is the molar density of air, V is the volume of the measurement system, and A is the area of the AC footprint. The accuracy of the AC method was estimated to be –12.5 % due to alteration of gas flow by the AC (Evans et al., 2001); precision is ± 10 % (Chiodini et al., 1998). Each AC measurement is typically made by one person within several minutes, allowing for many measurements to be made over relatively short periods of time under variable terrain conditions. The cost of the portable AC instrumentation typically ranges from ~\$15,000 to \$25,000.

5.3. Eddy covariance method

Eddy covariance (EC) (Baldocchi, 2003 and references therein) is a technique whereby high-frequency measurements of atmospheric CO_2 concentration at a fixed height above ground are made by an IRGA, along with micrometeorological variables such as wind velocity, temperature, and relative humidity (Fig. 5). Integration of these measurements provides a gross conservation of energy and mass over an area of land (the EC footprint) from which the net CO_2 flux is derived. The method essentially involves time averaging the product of the time series of fluctuating CO_2 concentration and vertical wind velocity. Under steady-state conditions and for sufficiently long averaging time, this converges to the ensemble mean flux. The measured vertical CO_2 flux is an integral of the surface flux over the upwind footprint (typically m^2 to km^2), the size of which scales with the measurement height, and is also dependent on meteorological conditions. One advantage of EC is that it provides a spatially and temporally averaged measurement, potentially providing more representative flux data and allowing for more efficient monitoring strategies than point measurements can provide. A limitation of the EC method is that it assumes a horizontal and homogeneous surface, and violations of this assumption can introduce significant error into the measurement. However, under acceptable terrain and meteorological conditions, estimates of daytime and nighttime error are generally less than 7 and 12%, respectively (e.g., Moore, 1986; Soegaard et al., 2000; Berger et al., 2001). The cost of EC equipment can range from ~\$15,000 to \$40,000.

6. Strategies for detection of geothermal CO_2

To meet the challenge of detecting potentially small-magnitude geothermal CO_2 emissions within the natural background variability of CO_2, we propose an approach that integrates available detection and monitoring techniques with statistical analysis and modeling strategies. Overall, we advocate a monitoring strategy that initially focuses on rapid, economical, reliable measurements of CO_2 concentrations in the soil and potentially in pre-existing wells and/or gradient holes within the study area, and surface CO_2 fluxes using the AC method. Our objective is to minimize the number of these measurements and then focus more time- and cost-intensive methods on "high-probability" anomalies of geothermal origin.

Even small geothermal source CO_2 fluxes are expected to produce high CO_2 concentrations within the vadose zone (see Section 3). As a result, if wells and/or gradient holes already exist within the area targeted for geothermal exploration, they should be sampled for CO_2 concentration. These measurements may be particularly useful because they will be made at sub-soil depths where background CO_2 input is usually lower than within the soil zone. If elevated CO_2 concentrations are measured within wells or gradient holes, further geochemical analyses (e.g., isotopic) should be conducted to determine the CO_2 source. Point measurements of soil CO_2 fluxes and concentrations should also be made along grids using the AC method and a portable IRGA, respectively. These measurements should be repeated at (at least) one site within the study area to characterize diurnal variation. If the study area satisfies the terrain requirements of the EC technique and the project budget permits, EC should be used to measure net surface fluxes. Importantly, using any of the above-mentioned techniques, particular attention should be paid to characterizing gas flow along pathways that are highly permeable to gas flow from depth to the near surface, such as faults and fractures. For example, soil CO_2 concentrations and fluxes should be made within grids along fault/fracture zones at close sample spacing to characterize the spatial distribution and magnitude of CO_2 signals associated with these areas.

To obtain a baseline data set against which potential anomalous geothermal CO_2 emissions can be compared, the spatial and temporal variability of soil CO_2 fluxes and concentrations should also be quantified within a background area with similar geologic, climatic, and ecosystem characteristics to the area targeted for geothermal exploration. Bayesian statistical analysis of CO_2 concentration and flux measurements in both the area targeted for geothermal exploration and the background study area should be used to identify the presence (or absence) of CO_2 anomalies with high statistical confidence, and estimate the number of measurements required to do this (e.g., Bayes, 1763; Lewicki and Oldenburg, 2004). Also, geostatistical methods should be used to map the spatial distribution of soil CO_2 concentrations and fluxes, and these parameters' autocorrelation and cross-correlation coefficients. These maps can be used to discern spatial patterns that may be indicative of geothermal CO_2 emissions and estimate total CO_2 emission rates from the study areas (e.g., Lewicki et al., 2005).

Once CO_2 concentrations and fluxes have been determined to be anomalous with high statistical confidence, more expensive sampling of gas profiles with depth through the vadose zone, and chemical and isotopic analyses could be undertaken. In particular, an increase in CO_2 concentration with depth would indicate deep CO_2 emissions. Also, the carbon-13 and carbon-14 values of subsurface CO_2 should distinguish CO_2 of geothermal from background origin. Integrated analysis of all measurements can be used to determine if CO_2 derived from a deep geothermal source is present, and if so, the spatial extent of the anomaly.

7. Conclusions

The properties of CO_2, methods for detection and monitoring of this gas, and the ranges of natural background CO_2 fluxes and concentrations are generally well known. We are also able to gain some insight into expected near-surface CO_2 concentrations and fluxes resulting from CO_2 migration and seepage from hidden geothermal reservoirs using numerical simulation. In particular, modeling suggests that shallow subsurface CO_2 concentrations can become very large even for modest CO_2 fluxes, and that mean surface winds are very effective at dispersing CO_2 emissions. Nevertheless, detecting small anomalous geothermal CO_2 fluxes and concentrations within natural background CO_2 variations poses a challenge. The exploration strategy that we propose to find geothermal CO_2 involves integrated measurement and statistical analysis to understand the natural background system. Once this understanding is achieved, integrated measurement, modeling, and sampling technologies can be applied toward the characterization of CO_2 within the study area targeted for exploration. If CO_2 concentrations and fluxes are suggestive of the presence of CO_2 derived from a geothermal source, the area should be investigated further by more cost- and time-intensive vertical profile sampling and isotopic analyses. Integrated analysis of all measured data can be used to determine if CO_2 derived from a deep geothermal source is present, and if so, the spatial extent of the anomaly. The appropriateness of further geophysical measurements, installation of deep wells, and geochemical analyses of deep fluids can then be decided based on the results of the near surface CO_2 monitoring program.

Acknowledgements

This work was supported by the Assistant Secretary for Energy Efficiency and Renewable Energy, Office of Geothermal Technologies, of the U.S. Department of Energy, and by the Office of Science, U.S. Department of Energy, under Contract No. DE-AC03-76SF00098. We thank C. Doughty (LBNL) and B.M. Kennedy (LBNL) for constructive reviews of this paper.

References

Alexander, M., 1977. Introduction to Soil Microbiology, 2nd ed. John Wiley and Sons, New York.

Amundson, R.G., Davidson, E.A., 1990. Carbon and nitrogeneous gases in the soil atmosphere. J. Geochem. Explor. 38, 13-41.

Amundson, R.G. Smith, V.S., 1988. Annual cycles of physical and biological properties in an uncultivated and irrigated soil in the San Joaquin Valley of California. Agriculture, Ecosystems, Env., 20, 195–208.

Arya, S.P., 1999. Air Pollution Meteorology and Dispersion. Oxford University Press.

Baldocchi, D., 2003. Assessing the eddy covariance technique for evaluating carbon dioxide exchange rates of ecosystems: past present, and future. Global Change Biology, 9, 479-492.

Bayes, T., 1763. An essay towards solving a problem in the doctrine of chances. Phil. Trans. Royal Soc. Lond., 53, 370–418.

Berger, B.W., Davis, K.J., Yi, C., Bakwin, P.S., Zhao, C., 2001. Long-term carbon dioxide fluxes from a very tall tower in a northern forest: flux measurement methodology. J. Atm. Ocean Technol., 18, 529-542.

Bergfeld, D., Goff, F., Janik, C.J., 2001. Elevated carbon dioxide flux at the Dixie Valley geothermal field, Nevada; relations between surface phenomena and the geothermal reservoir. Chem. Geol., 177, 43-66.

Cardellini, C., Chiodini, G., Frondini, F., Granieri, D., Lewicki, J., Peruzzi, L., 2003. Accumulation chamber measurements of methane fluxes: application to volcanic-geothermal areas and landfills. Appl. Geochem., 18, 45-54.

Chiodini, G., Cardellini, C., Frondini, F., Granieri, D., Marini, L., Ventura, G., 2001. CO_2 degassing and energy release at Solfatara volcano. Campi Flegrei, Italy, J. Geophys. Res., 106, 16,213–16,221.

Chiodini, G., Cioni, G. R., Guidi, M., Raco, B., Marini, L., 1998. Soil CO_2 flux measurements in volcanic and geothermal areas. Appl. Geochem., 13, 543–552.

Cruz, J.V., Couthinho, R.M., Carvalho, M.R., Oskarrson, N., Gislason, S.R., 1999. Chemistry of waters from Furnas volcano, Sao Miguel, Azores: fluxes of volcanic carbon dioxide and leached materials. J. Volcanol. Geotherm. Res., 92, 151-167.

Ellis, A.J. Mahon, W.A.J., 1977. Chemistry and Geothermal Systems. Academic Press, New York.

Evans, W. C., Sorey, M.L., Cook, A.C., Kennedy, B.M., Shuster, D.L., Colvard, E.M., White, L.D., Huebner, M.L. 2002. Tracing and quantifying magmatic carbon discharge in cold groundwaters: lessons learned from Mammoth Mountain, USA. J. Volcanol. Geotherm. Res., 114, 291–312.

Evans, W.C., Sorey, M.L., Kennedy, B.M., Stonestrom, D.A., Rogie, J.D., Shuster, D.L., 2001. High CO_2 emissions through porous media: Transport mechanisms and implications for flux measurement and fractionation. Chem. Geol., 177, 15-29.

Favara, R., Giammanco, S., Inguaggiatio, S., Pecoraino, G. 2001. Preliminary estimate of CO_2 output from Pantelleria Island volcano (Sicily, Italy): evidence of active mantle degassing. Appl. Geochem., 16, 883-894.

Gerlach, T.M., Doukas, M.P., McGee, K.A., Kessler, R., 2001, Soil efflux and total emission rates of magmatic CO_2 at the Horseshoe Lake tree kill, Mammoth Mountain, California. Chem. Geol., 177, 101-116.

Hernandez, P.A., Salazar, J.M., Shimoike, Y., Mori, T., Notsu, K., Perez, N., 2001. Diffuse emission of CO_2 from Miyakejima volcano, Japan. Chem. Geol., 177, 175-185.

Hinkle, M.E., 1994. Environmental conditions affecting concentrations of He, CO_2, O_2, and N_2 in soil gases. Appl. Geochem., 9, 53–63.

Klusman, R.W., Moore, J.N., LeRoy, M.P., 2000. Potential for surface gas flux measurements in exploration and surface evaluation of geothermal resources, Geothermics. 29, 637-670.

Koepenick, K.W., Brantley, S.L., Thompson, J.M., Rowe, G.L., Nyblade, A.A., Moshy, C., 1996. Volatile emissions from the crater and flank of Oldoinyo Lengai volcano, Tanzania. J. Geophys. Res., 101, 13,819-13,830.

Kucera, C.L., Kirkham, D.L., 1971. Soil respiration studies in tallgrass prairie in

Missouri. Ecology, 52, 912–915.

Lewicki, J.L. Oldenburg, C.M., 2004. Strategies for detecting hidden geothermal systems by near-surface gas monitoring. Lawrence Berkeley National Laboratory Report LBNL-56895.

Lewicki, J.L. Bergfeld, D., Cardellini, C., Chiodini, G., Granieri, D., Varley, N., Werner, C., in press, 2005. Comparative soil CO_2 flux measurements and geostatistical estimation methods on Masaya volcano, Nicaragua. Bull. Volcanol.

Lewicki, J.L., Connor, C., St-Amand, K., Stix, J., Spinner, W., 2003a. Self-potential, soil CO_2 flux, and temperature on Masaya volcano, Nicaragua. Geophys. Res. Lett., 30, 1817.

Lewicki, J.L., Evans, W.C. Hilley, G.E., Sorey, M.L., Rogie, J.D., Brantley, S.L., 2003b. Shallow soil CO_2 flow along the San Andreas and Calaveras faults, California. J. Geophys. Res., 108, ECV 3-1 – ECV 3-14.

Massmann, J., and D. Farrier, 1992. Effects of atmospheric pressures on gas transport in the vadose zone. Water Resour. Res., 28, 777–791.

Moore, C.J., 1986. Frequency response corrections for eddy covariance systems. Bound. Layer Meteorol., 37, 17-35.

Oldenburg, C.M., Unger, A.J.A., 2004. Coupled vadose zone and atmospheric surface-layer transport of CO_2 from geologic carbon sequestration seepage simulation. Vadose Zone J., 3, 848–857.

Osozawa, S., Hasegawa, S., 1995. Diel and seasonal changes in carbon dioxide concentration and flux in an andisol. Soil Science, 160, 117–124.

Pruess, K., Oldenburg, C., Moridis, G., 1999. TOUGH2 User's Guide Version 2.0.

Lawrence Berkeley National Laboratory Report LBNL-43134.

Schery, S. D., Gaeddert, D.H., Wilkening, M.H., 1984. Factors affecting exhalation of radon from a gravelly sandy loam. J. Geophys. Res., 89, 7299–7309.

Soegaard, H., Nordstroem, C., Friborg, T., Hansen, B.U., Christensen, T.R., Bay, C., 2000. Trace gas exchange in a high-arctic valley, 3. Integrating and scaling CO_2 fluxes from canopy to landscape using flux data, footprint modeling, and remote sensing. Glob. Biogeochem. Cycles, 14, 725-744.

Sorey, M.L., Evans, W.C., Kennedy, B.M., Farrar, C.D., Hainsworth, L.J., Hausback, B., 1998. Carbon dioxide and helium emissions from a reservoir of magmatic gas beneath Mammoth Mountain. California, J. Geophys. Res., 103, 15,303-15,323.

van Genuchten, M.T., 1980. A closed-form equation for predicting the hydraulic conductivity of unsaturated soils. Soil Sci. Soc. Am. J., 44, 892–898.

Werner, C., Brantley, S.L., Boomer, K., 2000. CO_2 emissions related to the Yellowstone volcanic system 2. Statistical sampling, total degassing, and transport mechanisms. J. Geophys. Res., 105, 10,831-10,846.

Wiant, H.V., 1967a. Influence of temperature on the rate of soil respiration. J. For., 65, 489–490.

Wiant, H.V., 1967b. Influence of moisture content on the “soil respiration”. J. For., 65, 902–903.

Williams-Jones, G., Stix, J., Heiligmann, M., Charland, A., Sherwood Lollar, B., Arner, N., Garzon, G., Barquero, V.J., Fernandez, E., 2000. A model of diffuse degassing at three subduction-related volcanoes. Bull. Volcanol., 62, 130-142.

Wood, W.W. Petraitis, M.J., 1984. Origin and distribution of carbon dioxide in the unsaturated zone of the southern high plains of Texas. Water Resour. Res., 20, 1193–

1208.

Wood, B.D., Keller, C.K., Johnstone, D.L., 1993. In situ measurement of microbial activity and controls on microbial CO_2 production in the unsaturated zone. Water Resour. Res., 29, 647–659.

Table 1. Measured soil CO_2 fluxes and concentrations at selected locations.

Site	Maximum CO_2 flux (g m^{-2} d^{-1})	Average CO_2 flux (g m^{-2} d^{-1})	Maximum soil CO_2 conc. (vol.%)	References
Solfatara crater, Italy	75,000	1520	na	Chiodini et al., 2001; Cardellini et al., 2003
Poggio dell'Ulivo cold degassing area, Italy	22,000	3911	na	Cardellini et al., 2003
Poas volcano, Costa Rica	140	na	16	Williams Jones et al., 2000
Arenal volcano, Costa Rica	291	na	7	Williams Jones et al., 2000
Masaya volcano, Nicaragua	50,000	na	na	Lewicki et al., 2003a
Oldoinyo Lengai volcano, Tanzania	1350	166	90	Koepenick et al., 1996
Yellowstone volcanic system, USA	30,000	Travertine areas: 89 Acid sulfate areas: 1200	90	Werner et al., 2000
Dixie Valley Geothermal Field, USA	570	na	na	Bergfeld et al., 2001
Mammoth Mountain, USA	>10,000	1500-2100	90	Gerlach et al., 2001; Sorey et al., 1998
Miyakejima volcano, Japan	18,150	na	na	Hernandez et al., 2001

Table 2. Properties of the coupled subsurface–surface-layer model system.

Property	Value
Subsurface	
Subsurface region extent (x x y x z)	1 km x 1 m x 124 m
Discretization (Nx x Ny x Nz)	67 x 1 x 31
Standard deviation of log k	0.70
Minimum, maximum k	1×10^{-14},1×10^{-10} m^2
Correlation length of k in X-, Z-direction	45, 1 m
Porosity (ϕ)	0.2
Infiltration rate (i)	0. cm yr^{-1}
Temperature (isothermal)	15^oC
CO_2 source location (x, y)	293.5 m, -86 m
Source CO_2 migration rate	1. x 10^{-4}, 1. x 10^{-5}, 1. x 10^{-6} kg s^{-1}
Residual water sat. (S_{lr})	0.1
Residual gas sat. (S_{gr})	0.01
van Genuchten (1980) α	1 x 10^{-4} Pa^{-1}
van Genuchten (1980) m	0.2
Surface Layer	
Surface-layer region extent (x x y x z)	1 km x 1 m x 62 m
Discretization (Nx x Ny x Nz)	67 x 1 x 31
Pressure in surface layer	1 bar
Temperature	15 ^oC
Velocity profile	Logarithmic
Reference velocity at z = 10 m	1 or 3 m s^{-1}
Friction velocity for v = 1 m s^{-1}	0.0861 m s^{-1}
Friction velocity for v = 3 m s^{-1}	0.261 m s^{-1}
Roughness length (z_0)	0.1 m

Table 3. Chemical and isotopic signatures related to CO_2 derived from different sources.

CO_2 source	$\delta^{13}C_{CO2}$ (‰)	$\Delta^{14}C_{CO2}$ (‰)	Near-surface CO_2 conc.	CO_2 conc. profile with depth	O_2 conc. profile with depth
Atmosphere	-7	70	Low	na	na
Plant root respiration and oxidative decay of young soil organic matter	C_3: -24 to –38 C_4: -6 to –19	≥70	Low to moderate	Increasing through soil zone	Decreasing through soil zone
Oxidative decay of ancient organic matter	C_3: -24 to –38 Aquatic/C_4: -6 to –19 Also age dependent	Highly depleted to absent, depending on age	Low	Potentially increasing through vadose zone	Potentially decreasing through vadose zone
Marine carbonate rocks	0 ± 4	Absent	Low	Increasing through vadose zone	No effect
Geothermal	-2 to -6	Absent	Moderate to high	Increasing through vadose zone	No effect

Conc., C_3, and C_4, refer to concentration, C_3 plants, and C_4 plants, respectively. All near-surface concentrations given are general estimates; they are strongly dependent on the magnitude of the CO_2 flux.

Figure Captions

Fig. 1. Conceptual model for gas migration from a deep hidden geothermal system. Also shown is the outline (dashed) of the two-dimensional model domain (see Fig. 2).

Fig. 2. Coupled CO_2 subsurface migration and surface-layer mixing at t = 200 years for one heterogeneous permeability realization, high source CO_2 flux (576 g m^{-2} d^{-1}), and constant wind speeds of 1 m s^{-1} (upper plot) and 3 m s^{-1} (lower plot). CO_2 concentration is in mole fraction. Dashed horizontal line shows ground surface.

Fig. 3. Horizontal profiles of shallow subsurface CO_2 concentration ([CO_2], 3 m depth) and surface CO_2 flux for low, medium, and high (5.76, 57.6, and 576 g m^{-2} d^{-1}, respectively) CO_2 source flux, one heterogeneous permeability realization, and t = 200 years.

Fig. 4. Schematic diagram of an accumulation chamber (AC) measurement system of soil CO_2 flux. The air contained in the AC is circulated through the AC and the infrared gas analyzer (IRGA) and the rate of change of CO_2 concentration in the AC is measured by the IRGA and recorded by the computer (PC).

Fig. 5. Schematic diagram of an eddy correlation (EC) instrumentation tower to measure surface CO_2 flux. An (A) open-path IRGA, (B) high frequency response sonic anemometer, and (C) box containing power source and datalogger/PC are shown.

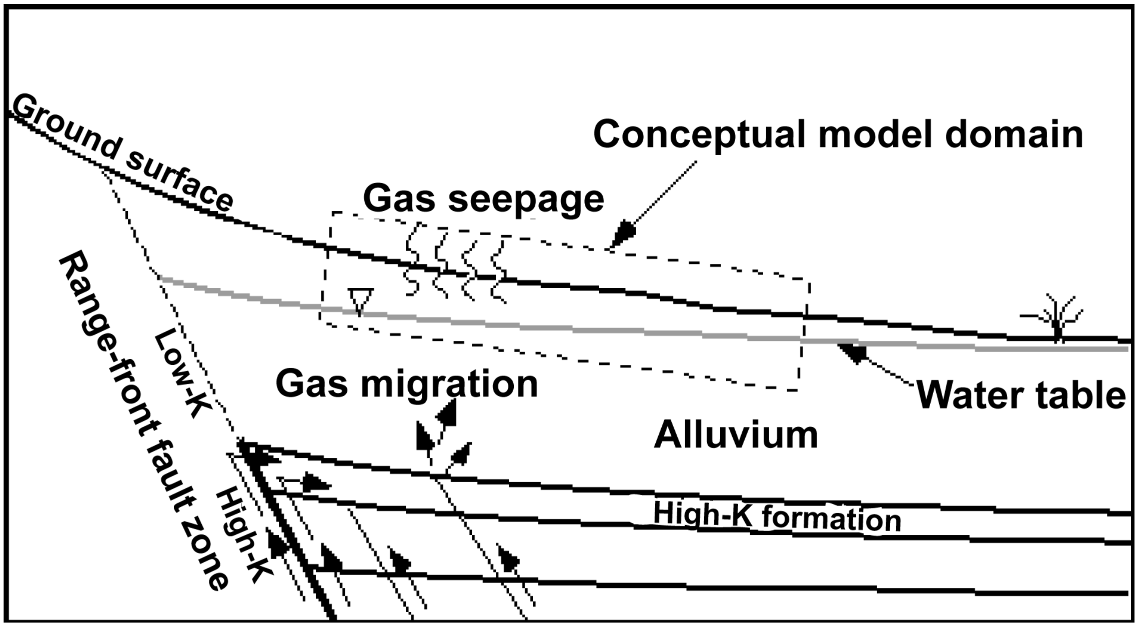
Ground surface
Conceptual model domain
Gas seepage
Range-front fault zone
Low-K
Gas migration
Water table
Alluvium
High-K
High-K formation

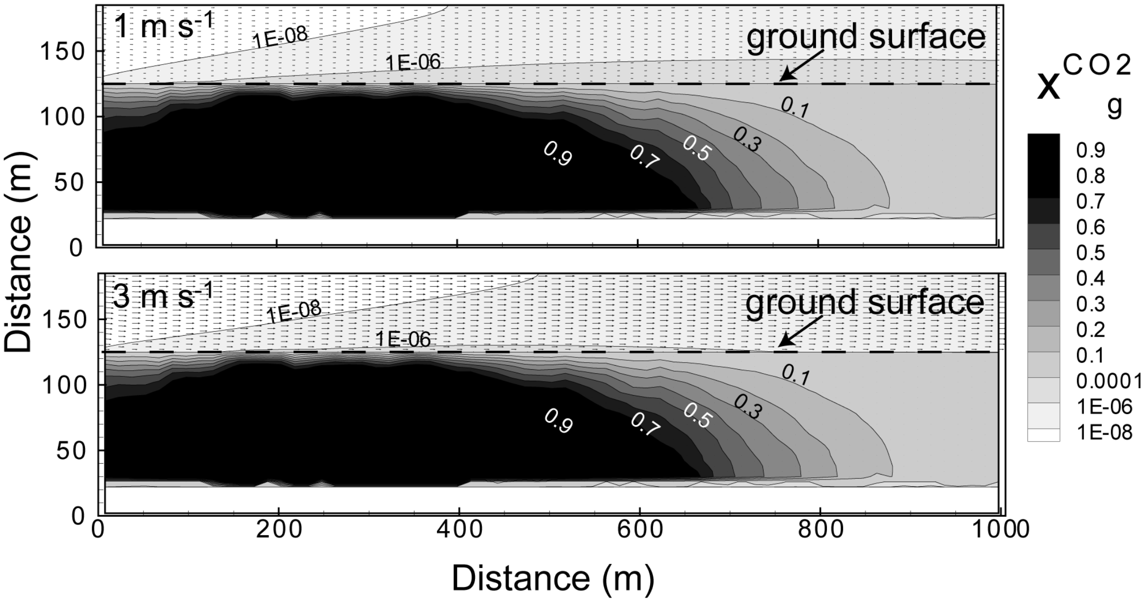
1 m s-1
3 m s-1
ground surface
1E-08
1E-06
0.9
0.7
0.5
0.3
0.1
Distance (m)
Distance (m)
x g CO2
0.9
0.8
0.7
0.6
0.5
0.4
0.3
0.2
0.1
0.0001
1E-06
1E-08
0
50
100
150
0
200
400
600
800
1000

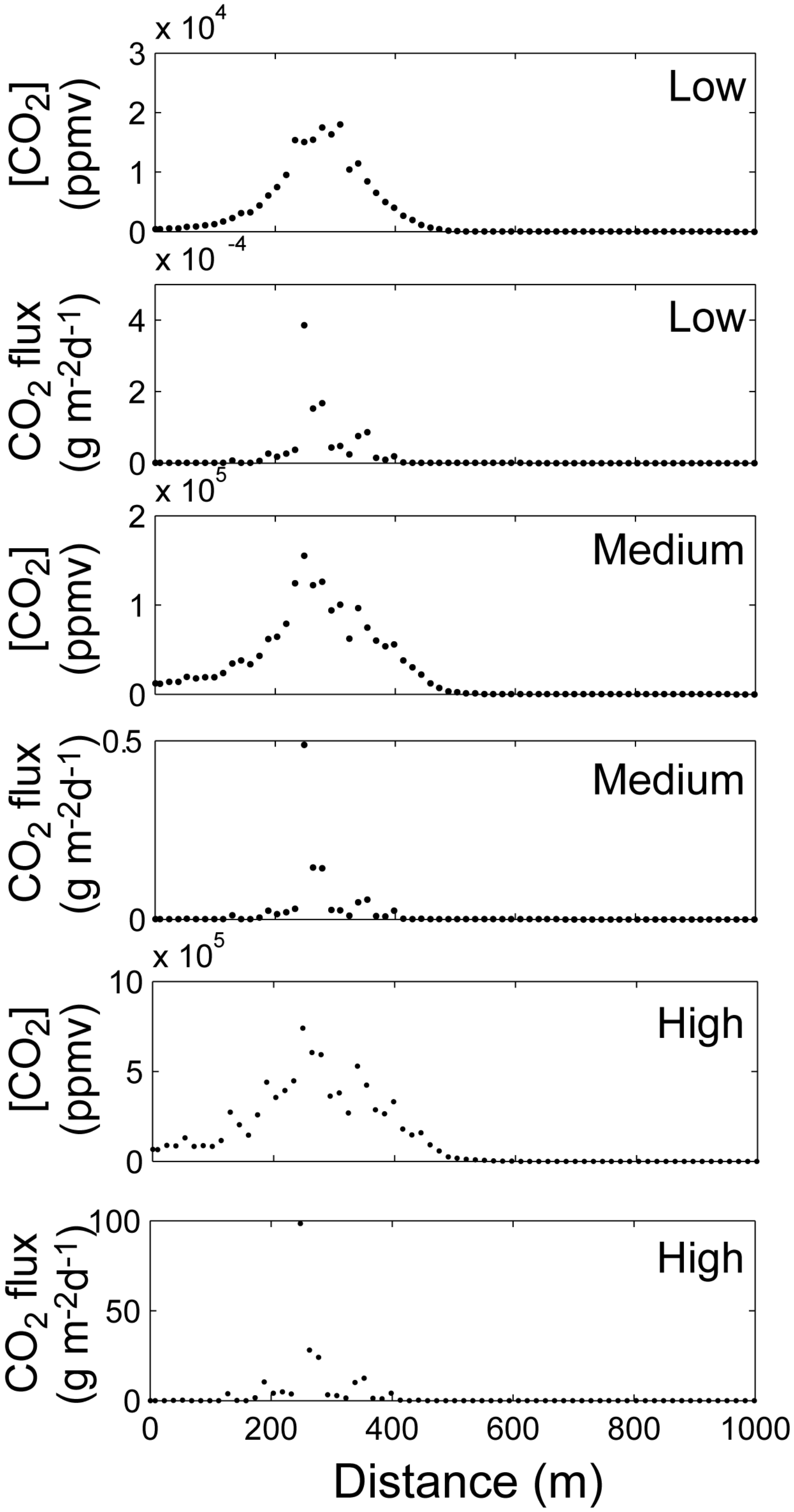
x 10^4
3
2
1
0
[CO2] (ppmv)
Low
x 10^-4
4
2
0
CO2 flux (g m-2d-1)
Low
x 10^5
2
1
0
[CO2] (ppmv)
Medium
0.5
0
CO2 flux (g m-2d-1)
Medium
x 10^5
10
5
0
[CO2] (ppmv)
High
100
50
0
CO2 flux (g m-2d-1)
High
0
200
400
600
800
1000
Distance (m)

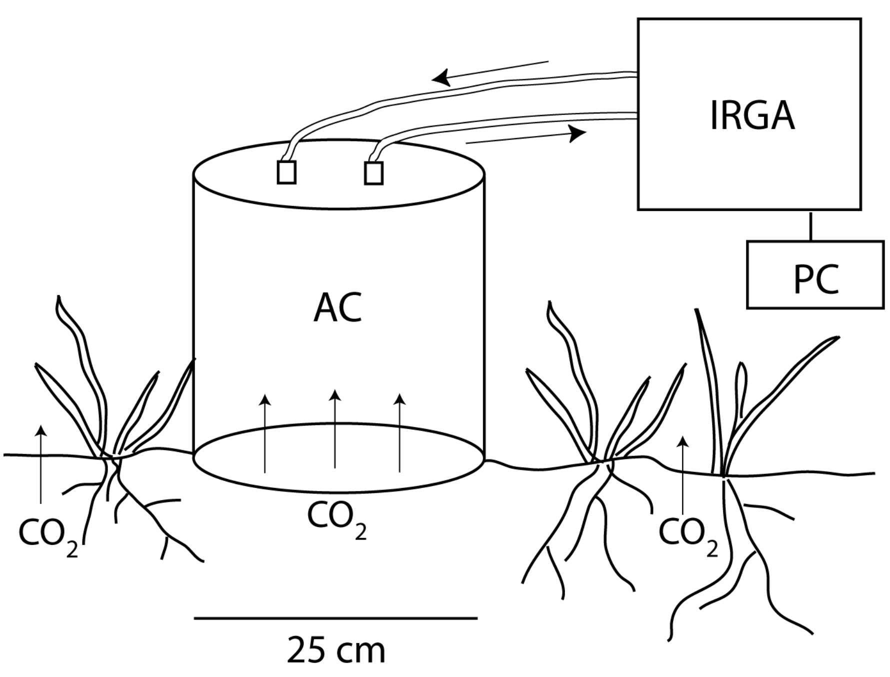
IRGA
PC
AC
CO_2
CO_2
CO_2
25 cm

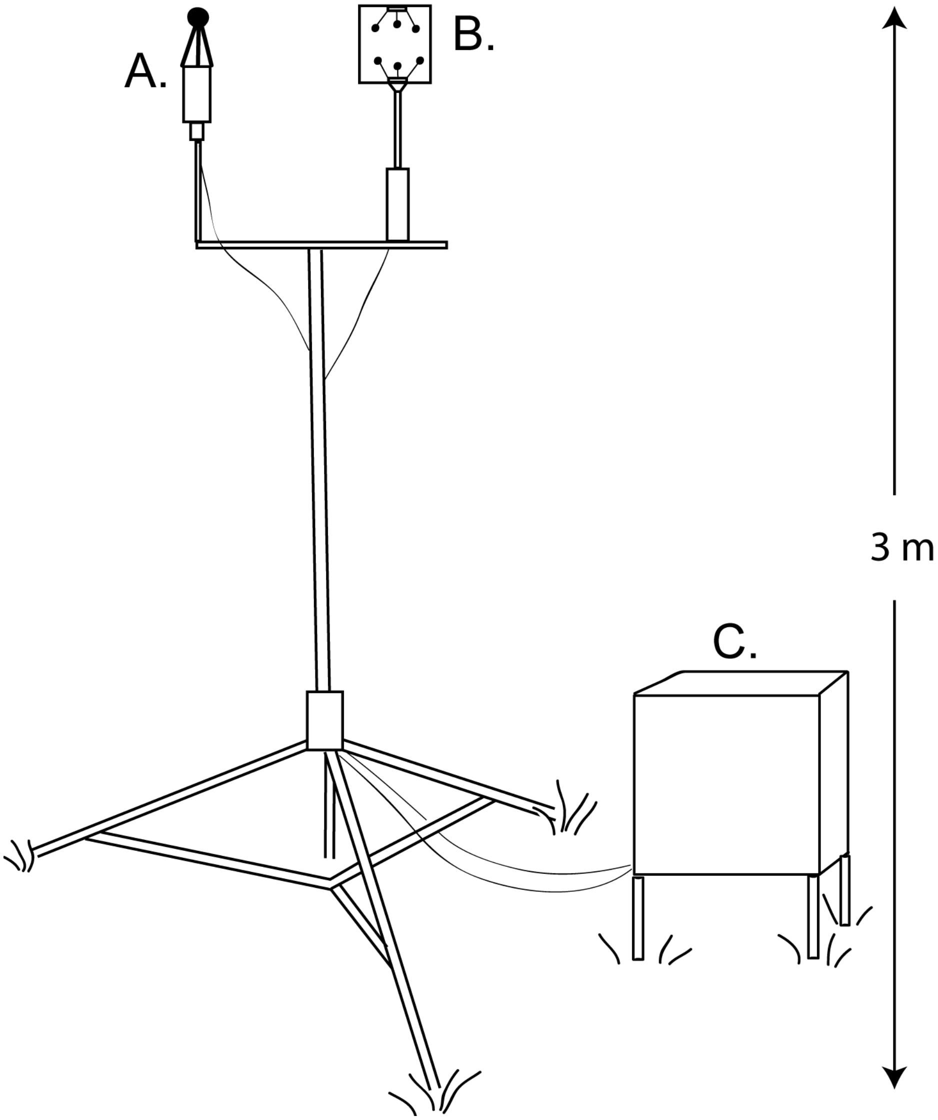
A.
B.
C.
3 m